DEVELOPMENTAL BIOLOGY

Germ line–inherited H3K27me3 restricts enhancer function during maternal-to-zygotic transition

Fides Zenk,[1,2] Eva Loeser,[1] Rosaria Schiavo,[1] Fabian Kilpert,[3] Ozren Bogdanović,[4,5,6] Nicola Iovino[1]*

Gametes carry parental genetic material to the next generation. Stress-induced epigenetic changes in the germ line can be inherited and can have a profound impact on offspring development. However, the molecular mechanisms and consequences of transgenerational epigenetic inheritance are poorly understood. We found that *Drosophila* oocytes transmit the repressive histone mark H3K27me3 to their offspring. Maternal contribution of the histone methyltransferase Enhancer of zeste, the enzymatic component of Polycomb repressive complex 2, is required for active propagation of H3K27me3 during early embryogenesis. H3K27me3 in the early embryo prevents aberrant accumulation of the active histone mark H3K27ac at regulatory regions and precocious activation of lineage-specific genes at zygotic genome activation. Disruption of the germ line–inherited Polycomb epigenetic memory causes embryonic lethality that cannot be rescued by late zygotic reestablishment of H3K27me3. Thus, maternally inherited H3K27me3, propagated in the early embryo, regulates the activation of enhancers and lineage-specific genes during development.

Although gametes are epigenetically reprogrammed upon fertilization to establish totipotency (*1*), environmentally induced chromatin changes in the germ line can be inherited and affect the offspring (*2*, *3*). DNA methylation, small regulatory RNAs, and histone modifications have been implicated as carriers of epigenetic information across generations. However, the mechanisms underlying transgenerational epigenetic inheritance and de novo establishment of the zygotic epigenome are poorly understood (*2*, *3*).

Polycomb group (PcG) proteins are thought to convey epigenetic memory in the late embryo by maintaining the repressed state of Hox cluster genes (*4*, *5*). PcG proteins also control multiple developmental processes (*5*) such as germ cell development (*6*, *7*). Enhancer of zeste [E(z)], the *Drosophila* homolog of vertebrate EZH1/2, is part of the Polycomb repressive complex 2 (PRC2) and catalyzes trimethylation of histone H3 Lys^{27} (H3K27me3). There is evidence that H3K27me3 may be germ line–inherited in some contexts (*8*–*10*) or may be reestablished during early embryogenesis (*11*–*13*). H3K27me3 can be inherited through the maternal and paternal germ lines in *Caenorhabditis elegans* (*14*), which undergo relatively little reprogramming during gametogenesis and at fertilization (*15*). Whether H3K27me3 intergenerational epigenetic inheritance occurs in other organisms that undergo drastic chromatin remodeling at fertilization is unclear. Further, the role of maternally supplied PRC2 in the early embryo remains unknown (*16*, *17*).

We investigated the distribution of H3K27me3 during gametogenesis in *Drosophila* and found that it was enriched in the oocyte in females (Fig. 1, A and B) but was strongly reduced in males during sperm differentiation, consistent with nucleosome replacement by protamines (fig. S1A). Although undetectable by immunofluorescence, some H3K27me3-marked histones are retained on mature sperm in *Drosophila* (*18*), similar to mouse, human, and zebrafish (*8*, *10*, *19*). Upon fertilization, H3K27me3 is still detectable in the maternal pronucleus at apposition, before the fusion of the two pronuclei (Fig. 1C, top, and fig. S1B).

To study early embryos devoid of maternally supplied *E(z)* mRNA and E(z) protein, we depleted E(z) at late stages of oogenesis (Fig. 1A). E(z)-knockdown [E(z)-KD] flies displayed reduced levels of *E(z)* mRNA (fig. S1C) and of endogenous E(z) protein (fig. S1D) in early embryos. E(z)-KD flies expressing a hemagglutinin-tagged E(z) [HA-E(z)] transgene driven by its endogenous promoter also displayed undetectable HA-E(z) in late oogenesis (Fig. 1B, right). However, H3K27me3 levels in oocytes were unaltered in E(z)-KD flies relative to wild-type flies (Fig. 1B and fig. S1E). Moreover, despite effective depletion of E(z) in early embryos, we could still detect H3K27me3 on the maternal pronucleus in E(z)-KD early embryos (Fig. 1C, bottom). Thus, H3K27me3 is transmitted maternally to the embryo and is not de novo reestablished at fertilization.

We found that inherited H3K27me3 was actively propagated from totipotent nuclei up to zygotic genome activation (ZGA) during early embryogenesis in wild-type embryos (Fig. 1, D and E, fig. S1F, and fig. S2, A to D), consistent with the nuclear localization of HA-E(z) (Fig. 1, F and G, and fig. S2B). In contrast, other histone modifications that we tested, including H3K27ac (acetylation), H3K4me1 (monomethylation of Lys^{4}), and H3K4me3, were de novo established later in the early embryo (fig. S2, E to G). Further, H3K27me3 was rapidly lost in E(z)-KD early embryos, after two or three nuclear divisions (Fig. 1E). Starting from cycle 6, HA-E(z) accumulated in nuclear foci resembling Polycomb bodies, which are typically observed at later developmental stages (Fig. 1F and fig. S2B) (*20*). Thus, maternally supplied E(z) is required to propagate inherited H3K27me3 during early embryogenesis.

To investigate H3K27me3 distribution during development, we performed chromatin immunoprecipitation sequencing (ChIP-seq) at precise stages in wild-type embryos (Fig. 2A), including totipotent nuclei (before cycle 9) (*21*), pluripotent nuclei (cycles 9 to 13, when about 100 genes are transcribed), and ZGA-stage embryos (cycle 14, when most genes are activated) (*22*) (Fig. 2B and fig. S2, H and I). H3K27me3 was already present on totipotent nuclei, consistent with immunofluorescence (Fig. 1D). We identified 32 H3K27me3-enriched domains that appear to be stable throughout embryonic development (from fertilization to ZGA) (Fig. 2, B and C, and database S1). Another 37 H3K27me3-enriched domains appeared specifically at ZGA (Fig. 2C). Most of the H3K27me3 reprogramming occurred between cycles 9 and 13 (pluripotent stage) (Fig. 2, B and C). H3K27me3 domains present in totipotent nuclei (before cycle 9) appear to be broader and less defined than those in later-stage embryos (Fig. 2D). In contrast, none of the H3K27me3-enriched domains were present in E(z)-KD embryos (Fig. 2B and database S1). Thus, Polycomb-mediated chromatin regulation occurs during early embryogenesis, even before zygotic transcription. Unexpectedly, the Hox cluster showed H3K27me3 enrichment long before segment formation (Fig. 2B), suggesting an inherited repressed state that is maintained or remodeled in a segment-dependent manner later in development (*23*).

As expected, E(z)-KD embryos displayed zygotic expression of *E(z)* mRNA at ZGA (Fig. 3A, green bar). However, none of the E(z)-KD embryos, including those generated with a different short hairpin RNA, completed embryogenesis (Fig. 3B and fig. S3, A and B). A large fraction of late-stage E(z)-KD embryos showed homeotic transformation, suggesting misregulation of Hox genes (fig. S3C). We investigated whether homeotic transformation arises from altered expression patterns of gap and pair-rule genes, which encode transcription factors that regulate segmentation and establish Hox gene expression (*24*). Indeed, E(z) was previously suggested to regulate the expression of the gap genes *knirps* and *giant* (*25*). However, none of the early segmentation genes displayed altered expression patterns in E(z)-KD embryos (fig. S3, D to H). These data suggest that intergenerationally inherited and pre-ZGA

[1]Department of Chromatin Regulation, Max Planck Institute of Immunobiology and Epigenetics, D-79108 Freiburg, Germany. [2]Faculty of Biology, University of Freiburg, D-79104 Freiburg, Germany. [3]Bioinformatics Facility, Max Planck Institute of Immunobiology and Epigenetics, D-79108 Freiburg, Germany. [4]Genomics and Epigenetics Division, Garvan Institute of Medical Research, Sydney, New South Wales, Australia. [5]St Vincent's Clinical School, Faculty of Medicine, University of New South Wales, Sydney, New South Wales, Australia. [6]ARC Centre of Excellence in Plant Energy Biology, University of Western Australia, Perth, Western Australia 6009, Australia.
*Corresponding author. Email: iovino@ie-freiburg.mpg.de

H3K27me3 are essential for correct Hox patterning later in development. Further, overexpression of *E(z)* from ZGA onward did not markedly improve the survival of embryos lacking H3K27me3 during early embryogenesis (fig. S3A). Overall, the data suggest that the lack of H3K27me3 and E(z) prior to ZGA cannot be rescued by the zygotic expression of *E(z)* (Fig. 3, A and B, and fig. S3, A to C), consistent with roles for maternal *extra sex combs* (*esc*/EED in vertebrates, another PRC2 component) and maternal Utx (the H3K27me3 demethylase, KDM6A in vertebrates) in Hox gene regulation during embryogenesis (*16*, *26*).

To confirm the E(z)-KD data, we used a well-established temperature-sensitive allele of *E(z)*, $E(z)^{61}$ [E(z)-TS] (*17*). E(z)-TS embryos raised at a nonpermissive temperature did not display H3K27me3 and did not complete embryonic development (Fig. 3, C and D). When E(z)-TS embryos were shifted to the permissive temperature at ZGA, the H3K27me3 levels were restored (Fig. 3D), mainly to the correct genomic locations (fig. S3, I and J). Thus, at least some of the cells or segments within the shifted E(z)-TS embryos could properly restore H3K27me3 in late embryogenesis. Of note, in E(z)-TS embryos raised at a nonpermissive temperature, H3K27me3 was sharply reduced throughout the genome (fig. S3K) but was not completely removed (fig. S3L), providing the opportunity to reestablish repressive chromatin domains through the aromatic cage domain of Esc (EED) and the subsequent recruitment of PRC2 (*27*). Despite the restoration of H3K27me3, 80% of the shifted E(z)-TS embryos did not complete embryonic development; of these, almost 50% showed homeotic transformations (Fig. 3E and fig. S3M). Hox genes were misexpressed starting from stage 9 or 10 (after gastrulation) (fig. S3, N and O), and the Hox gene *Abdominal-B* (*Abd-B*) was deregulated, despite the presence of H3K27me3 in the same embryo (fig. S3P).

In addition, we used a histone H3 $Lys^{27} \rightarrow$ Met mutant (H3K27M) that in *Drosophila* has been shown to phenocopy PRC2 loss of function (*28*). Maternal (pre-ZGA) and zygotic (post-ZGA) expression of H3K27M effectively reduced H3K27me3 levels, but only maternal H3K27M expression caused embryonic lethality (Fig. 3, F and G). Homeotic transformations, as well, were observed only when H3K27M was expressed from pre-ZGA onward (Fig. 3, H and I, and fig. S3Q). These data, together with the E(z)-KD and E(z)-TS data, further confirm that epigenetic regulation at the Hox cluster occurs during early embryonic development, before ZGA. We propose that H3K27me3 stabilizes an inherited, default-repressed chromatin state of the Hox cluster.

ZGA is characterized by de novo deposition of active histone marks, including H3K4me3, H3K27ac, H3K36me3, and H3K4me1, as well as by the active recruitment of RNA polymerase II to chromatin (*9*, *11*, *12*). We found that the absence of pre-ZGA H3K27me3 did not affect ZGA timing or RNA Pol II–Ser2P (phosphorylated RNA polymerase II) recruitment to chromatin (fig. S4, A and B).

Next, we evaluated the epigenome at ZGA in embryos that lacked pre-ZGA H3K27me3. We

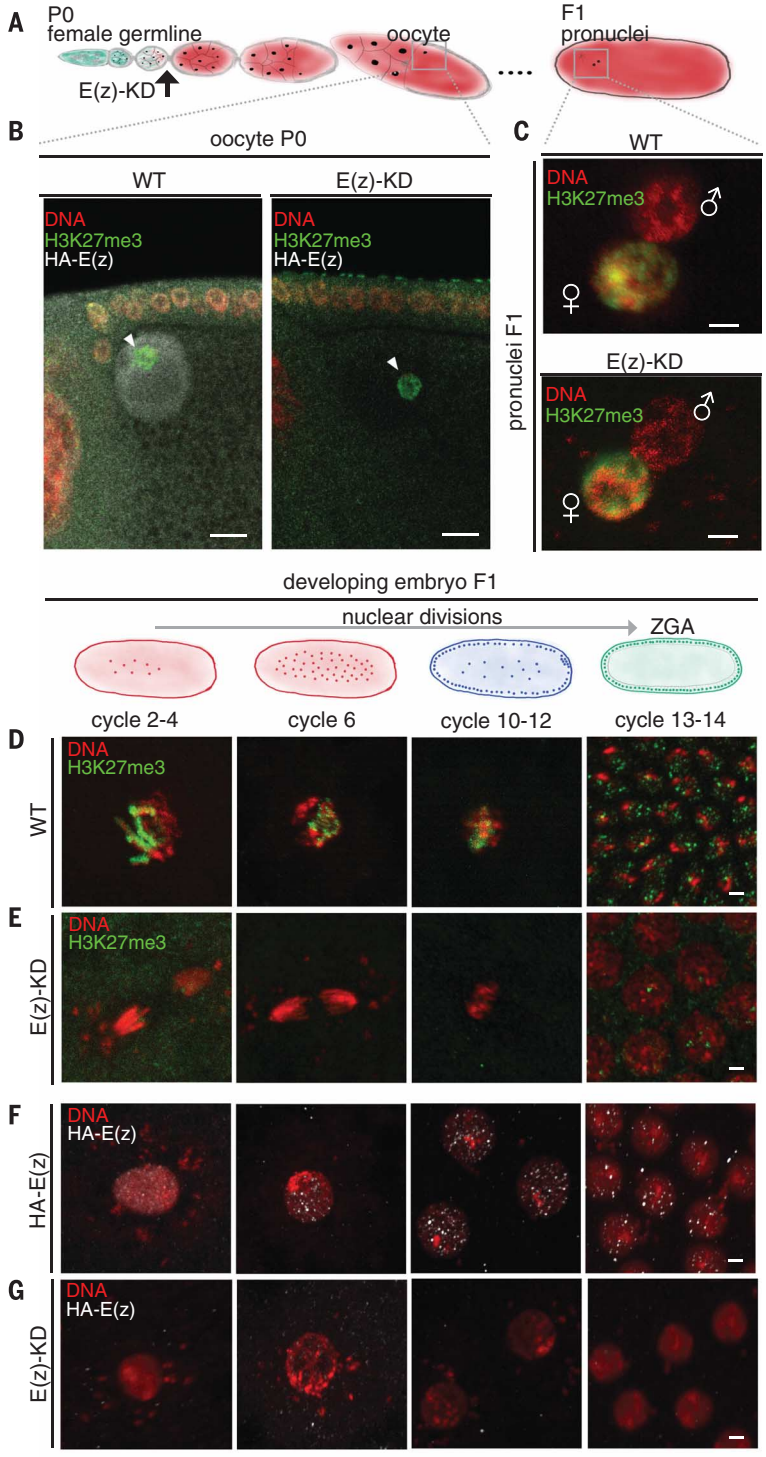

Fig. 1. Intergenerational inheritance of H3K27me3 from *Drosophila* oocyte. (**A**) Schematic of one ovariole in the germ line of a *Drosophila*. In red, regions of E(z)-KD (arrow). The right side of the cartoon depicts the apposition of maternal and paternal pronuclei. (**B**) Stage 10 egg chamber of a strain expressing HA-E(z). The H3K27me3 marks the oocyte (arrowhead). HA-E(z) is present in the nucleoplasm and on the chromatin of the wild-type oocyte. See fig. S1E. Scale bars, 10 μm. (**C**) Antibody to H3K27me3 (α-H3K27me3) and 4′,6-diamidino-2-phenylindole (DAPI) staining of the apposed pronuclei in one-cell wild-type and E(z)-KD embryos. H3K27me3 is also transmitted to the embryo on the maternal gamete in the absence of E(z). See fig. S1B. Scale bars, 2 μm. (**D**) α-H3K27me3 and DAPI staining of wild-type early embryos at different developmental cycles. For clarity, mitotic chromosomes are shown. See fig. S2, A and B. Scale bar, 2 μm (here and below). (**E**) α-H3K27me3 and DAPI staining of E(z)-KD embryos. (**F**) α-HA and DAPI staining of HA-E(z) strain in early embryos at different developmental cycles and at different phases of the cell cycle. (**G**) α-HA and DAPI staining of E(z)-KD embryos.

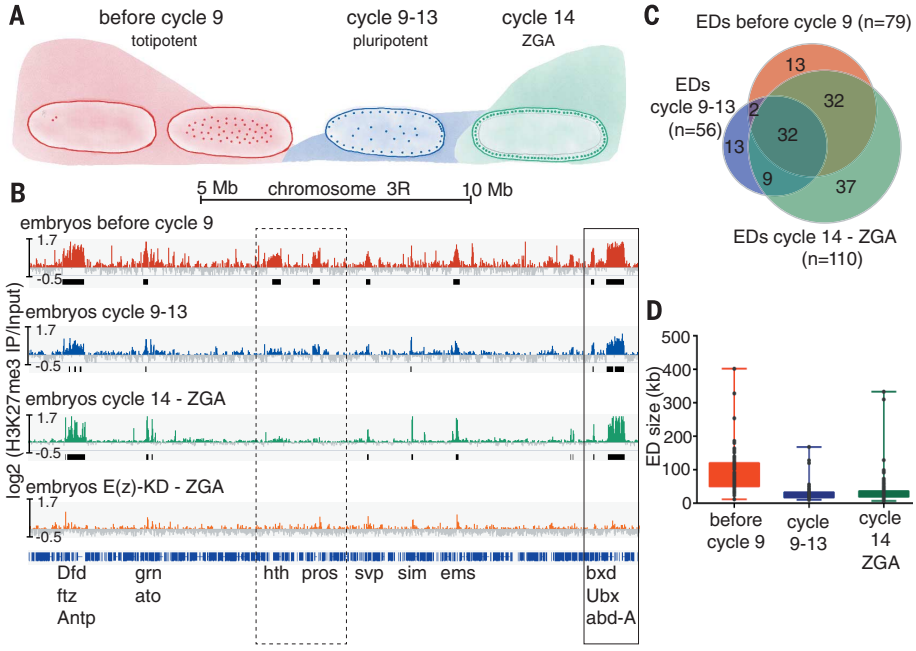

Fig. 2. Polycomb-mediated chromatin regulation during early embryogenesis, prior to ZGA. (**A**) Cartoon of early embryonic development of *Drosophila*. The number of cycles corresponds to the mitotic divisions. During cycles 9 to 13, an initial subset of 100 genes is transcribed (blue wave). After 14 mitotic divisions, the embryo is fully transcriptionally competent (green wave). (**B**) H3K27me3 ChIP-seq tracks. The Hox cluster (right inset) is already decorated with H3K27me3 before cycle 9. Other H3K27me3-marked regions lose the mark during development (left inset). The enriched H3K27me3 domains (EDs, false discovery rate = 0.05) are shown below each track in black. The last track shows the H3K27me3 signal in E(z)-KD embryos at ZGA. See also fig. S2I. (**C**) Venn diagram showing the total number and overlap of EDs detected at each developmental stage. (**D**) Box plot showing the size distribution (in kb) of the enriched domains.

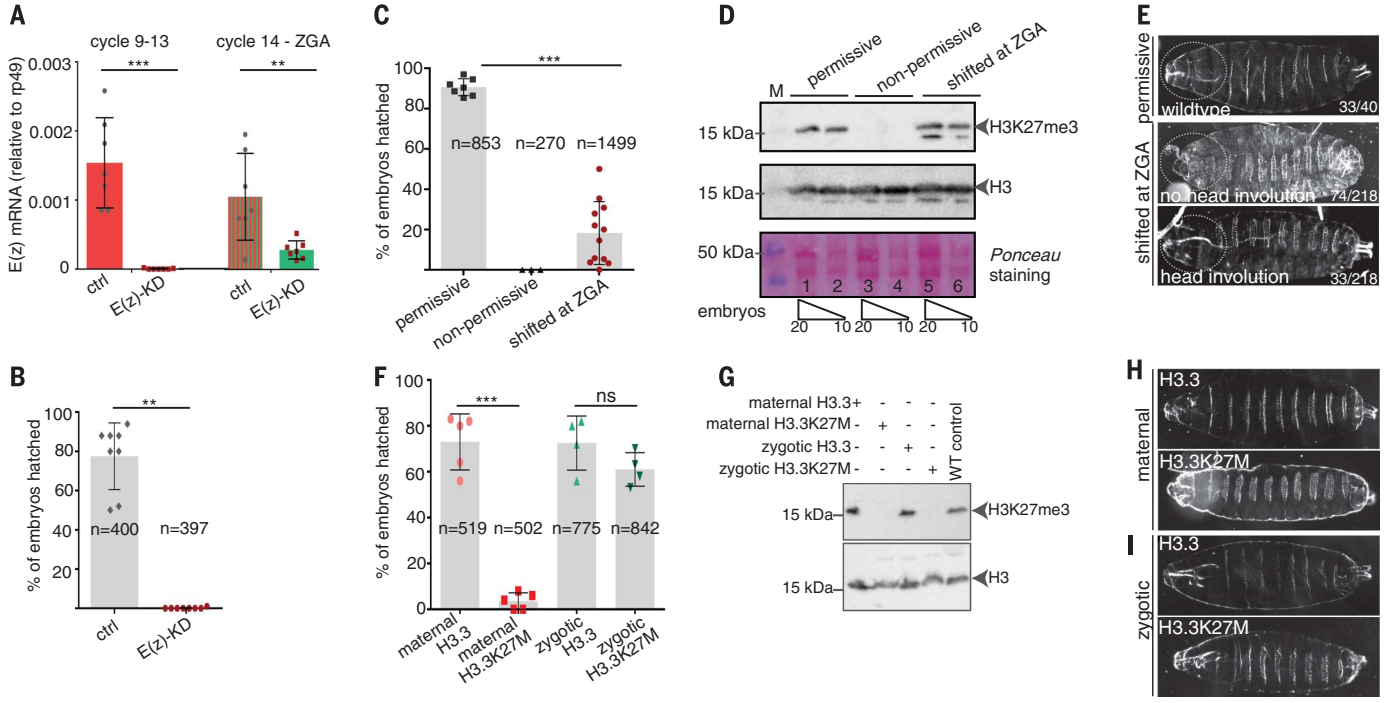

Fig. 3. Loss of H3K27me3 before zygotic genome activation leads to embryonic lethality and homeotic transformation. (**A**) *E(z)* mRNA levels were analyzed by quantitative reverse transcription polymerase chain reaction (qRT-PCR). Before ZGA (cycles 9 to 13), the maternally loaded mRNA (red) is strongly reduced upon E(z)-KD. At ZGA (cycle 14), *E(z)* mRNA (green) is zygotically transcribed in E(z)-KD embryos (cycles 9 to 13, $P = 4.4 \times 10^{-5}$; cycle 14, $P = 0.008$; *t* test). (**B**) Hatching rate of fertilized control and E(z)-KD eggs ($P = 0.0002$, Mann-Whitney test). See fig. S3, A to C. (**C**) Hatching rate of E(z)-TS embryos reared at a permissive temperature, at a nonpermissive temperature, and shifted to a permissive temperature from ZGA onward ($P < 0.0001$, Mann-Whitney test). (**D**) Total extracts of stage 17 (end of embryogenesis) embryos were analyzed by Western blot with α-H3K27me3. α-H3 and Ponceau staining were used as loading controls. H3K27me3 is detectable in shifted embryos, confirming that E(z) regains its enzymatic function (lanes 5 and 6). (**E**) Representative examples of cuticle preparations of embryos reared at a permissive temperature and of embryos shifted to a permissive temperature at ZGA showing homeotic transformations. See fig. S3M. (**F**) Hatching rate of embryos from fly strains overexpressing H3.3 and H3.3K27M transgenes. (maternal $P = 0.008$, zygotic $P = 0.2$; Mann-Whitney test). (**G**) Total extracts of stage 17 embryos were analyzed by Western blot with α-H3K27me3 upon overexpression of H3.3K27M. Both the maternal and zygotic H3.3K27M mutant transgenes strongly reduced H3K27me3. α-H3 was used as a loading control. (**H**) Representative examples of cuticle preparations of embryos with maternally overexpressed H3.3 or H3.3K27M. Maternal overexpression of H3.3K27M caused homeotic transformations. (**I**) Representative examples of cuticle preparations of embryos that express H3.3 or H3.3K27M zygotically (post-ZGA). The embryos do not develop homeotic transformations.

performed ChIP-seq for the active histone marks H3K27ac and H3K4me1 at ZGA in wild-type and E(z)-KD embryos. Heat maps centered on the H3K27ac peak summit revealed the de novo appearance of H3K27ac signals in E(z)-KD embryos (Fig. 4A, top, and fig. S4C), whereas H3K27ac signals were unaltered in other genomic regions (Fig. 4A, bottom, and fig. S4C). The de novo H3K27ac peaks in E(z)-KD embryos overlapped with regions that are strongly enriched for H3K27me3 in wild-type versus E(z)-KD embryos (Fig. 4A and fig. S4C); this finding suggests that pre-ZGA H3K27me3 prevents aberrant accumulation of active H3K27ac marks in neighboring domains at ZGA. H3K27ac marks are usually associated with active enhancers. Indeed, the de novo H3K27ac peaks acquired in E(z)-KD embryos fall into a large subclass of enhancers marked by H3K4me1 and H3K27me3 in wild-type embryos—a chromatin state associated with repressed or poised enhancers (Fig. 4A) (*29*, *30*). Moreover, 52 of the top 200 de novo H3K27ac peaks overlap with genomic sequences previously shown to function as transcriptional enhancers (fig. S4, D to G) (*31*).

We used a conservative approach to determine the closest gene to the top 200 de novo H3K27ac peaks gained in E(z)-KD embryos (the top 200 H3K27ac-associated genes; database S2). We hypothesized that the loss of pre-ZGA H3K27me3 and corresponding gain of H3K27ac triggers aberrant activation of poised enhancers, causing transcriptional defects. To test this hypothesis, we performed total RNA-seq of both wild-type and E(z)-KD embryos at different developmental stages, including at cycles 9 to 13 (pluripotent stage) and at cycle 14 (ZGA) (database S3). We found that the top 200 H3K27ac-associated genes were up-regulated specifically at ZGA in E(z)-KD embryos relative to wild-type embryos, and not at cycles 9 to 13. (Fig. 4B and fig. S4H). The spread of de novo H3K27ac overlapped with H3K27me3 depletion and transcriptional defects in E(z)-KD embryos, and with H3K4me1 regions in wild-type embryos, as exemplified for the region shown in Fig. 4C. Metaprofile analysis showed that H3K27ac levels increased specifically at the promoter regions of the top 200 associated genes in E(z)-KD embryos (fig. S4, I and J). We confirmed the relative transcriptional up-regulation and H3K27me3 depletion on a subset of genes in E(z)-KD embryos (Fig. 4, D and E, and fig. S4K). Thus, loss of maternally inherited E(z) and H3K27me3 leads to aberrant activation of a subset of genes at ZGA.

Gene ontology term analysis of the top 200 H3K27ac-associated genes showed a strong enrichment for embryonic patterning, segmentation, and other developmental programs (fig. S4L). We found that a subset of the top 200 de novo H3K27ac peaks identified in E(z)-KD embryos also accumulated H3K27ac in wild-type late embryos (fig. S4, M and N). Further, the top 200 H3K27ac-associated genes that are up-regulated at ZGA in E(z)-KD embryos were up-regulated in wild-type late embryos or adults, suggesting that E(z)-KD embryos display precocious activation of genes that are expressed at later stages in wild-type embryos and flies (fig.

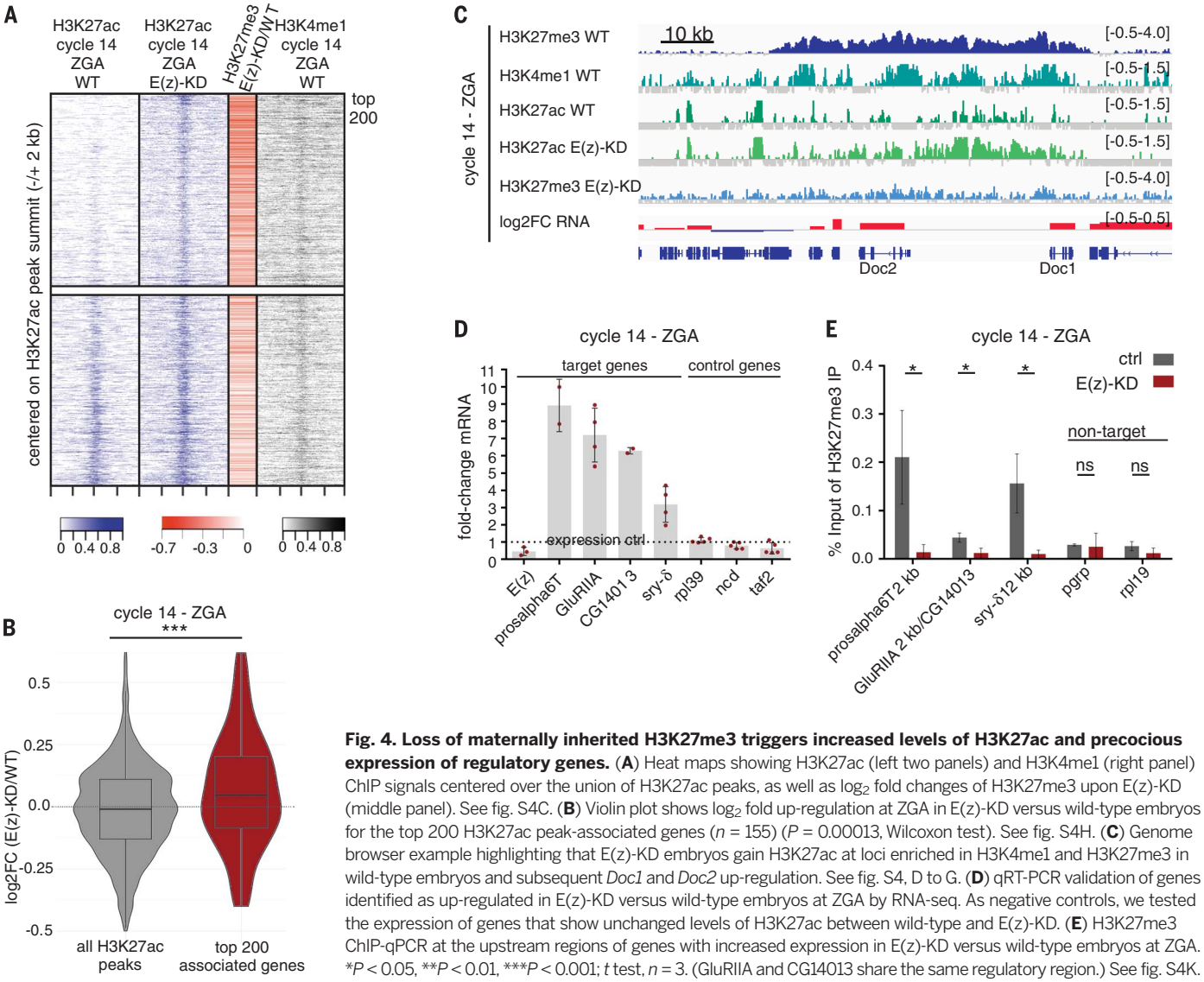

Fig. 4. Loss of maternally inherited H3K27me3 triggers increased levels of H3K27ac and precocious expression of regulatory genes. (**A**) Heat maps showing H3K27ac (left two panels) and H3K4me1 (right panel) ChIP signals centered over the union of H3K27ac peaks, as well as $\log_2$ fold changes of H3K27me3 upon E(z)-KD (middle panel). See fig. S4C. (**B**) Violin plot shows $\log_2$ fold up-regulation at ZGA in E(z)-KD versus wild-type embryos for the top 200 H3K27ac peak-associated genes (n = 155) (P = 0.00013, Wilcoxon test). See fig. S4H. (**C**) Genome browser example highlighting that E(z)-KD embryos gain H3K27ac at loci enriched in H3K4me1 and H3K27me3 in wild-type embryos and subsequent *Doc1* and *Doc2* up-regulation. See fig. S4, D to G. (**D**) qRT-PCR validation of genes identified as up-regulated in E(z)-KD versus wild-type embryos at ZGA by RNA-seq. As negative controls, we tested the expression of genes that show unchanged levels of H3K27ac between wild-type and E(z)-KD. (**E**) H3K27me3 ChIP-qPCR at the upstream regions of genes with increased expression in E(z)-KD versus wild-type embryos at ZGA. *P < 0.05, **P < 0.01, ***P < 0.001; t test, n = 3. (GluRIIA and CG14013 share the same regulatory region.) See fig. S4K.

S4O). We also observed H3K27ac spreading at the Hox cluster (fig. S5A), which suggests that loss of pre-ZGA H3K27me3 and accumulation of H3K27ac resulted in altered chromatin states at this locus and caused the transcriptional defects later in development (fig. S3N). The accumulation of H3K27ac at the Hox cluster in E(z)-TS embryos was not reversed after shifting the embryos to the permissive temperature at ZGA, consistent with persistent homeotic transformation and lethality (Fig. 3, C to E, and fig. S5A). Thus, maternally inherited and pre-ZGA H3K27me3 restricts lineage-specific gene expression and regulatory regions by preventing their precocious activation at ZGA.

Our results indicate that H3K27me3 is intergenerationally inherited from the maternal germ line and resists reprogramming events during early embryogenesis in *Drosophila*. At lower levels, H3K27me3 is also retained in mature sperm, which suggests that epigenetic information carried by modified histones is also contributed to the zygote paternally (*2*, *3*, *8*, *10*, *19*). Propagation of germ line–inherited H3K27me3 by maternally supplied PRC2 prevents the aberrant spread of active histone marks and ectopic expression of lineage regulators at ZGA. Our data suggest that a Polycomb-based chromatin signature represses and poises early developmental enhancers at ZGA. PRC1 was shown to be required only after ZGA (*32*). Therefore, although PRC1 has also been shown to be retained through DNA replication and potentially provide maintenance of transcriptional silencing through cell division (*33*), we suggest that the Polycomb intergenerational epigenetic memory of repressed states is propagated solely through the H3K27me3 mark. We also show that the Hox cluster resides in a repressed chromatin state, marked by H3K27me3, throughout early embryogenesis until its chromatin is remodeled in a segment-specific manner later in development (*23*), as suggested for vertebrates (*34*). Therefore, the epigenetic memory imposed by PRC2 is germ line–inherited and appears to function much earlier than previously appreciated (*5*). H3K27me3 was recently shown to be present on pre-implantation embryo chromatin in mouse; we speculate that H3K27me3 could have similar functions during mammalian embryogenesis (*35*). We further propose that environmentally induced alterations of histone modifications in the adult germ line could contribute to transgenerational epigenetic inheritance.

REFERENCES AND NOTES

1. H. D. Morgan, F. Santos, K. Green, W. Dean, W. Reik, *Hum. Mol. Genet.* **14** (suppl. 1), R47–R58 (2005).
2. E. A. Miska, A. C. Ferguson-Smith, *Science* **354**, 59–63 (2016).
3. U. Sharma, O. J. Rando, *Cell Metab.* **25**, 544–558 (2017).
4. J. A. Simon, R. E. Kingston, *Nat. Rev. Mol. Cell Biol.* **10**, 697–708 (2009).
5. U. Grossniklaus, R. Paro, *Cold Spring Harb. Perspect. Biol.* **6**, a019331 (2014).
6. N. Iovino, F. Ciabrelli, G. Cavalli, *Dev. Cell* **26**, 431–439 (2013).
7. W. Mu, J. Starmer, A. M. Fedoriw, D. Yee, T. Magnuson, *Genes Dev.* **28**, 2056–2069 (2014).
8. U. Brykczynska *et al*., *Nat. Struct. Mol. Biol.* **17**, 679–687 (2010).
9. S. Hontelez *et al*., *Nat. Commun.* **6**, 10148 (2015).
10. S. S. Hammoud *et al*., *Nature* **460**, 473–478 (2009).
11. X. Y. Li, M. M. Harrison, J. E. Villalta, T. Kaplan, M. B. Eisen, *eLife* **3**, 03737 (2014).
12. N. L. Vastenhouw *et al*., *Nature* **464**, 922–926 (2010).
13. H. Zheng *et al*., *Mol. Cell* **63**, 1066–1079 (2016).
14. L. J. Gaydos, W. Wang, S. Strome, *Science* **345**, 1515–1518 (2014).
15. M. Samson *et al*., *PLOS Genet.* **10**, e1004588 (2014).
16. G. Struhl, D. Brower, *Cell* **31**, 285–292 (1982).
17. R. S. Jones, W. M. Gelbart, *Genetics* **126**, 185–199 (1990).
18. A. H. Elnfati, D. Iles, D. Miller, *Genom. Data* **7**, 175–177 (2015).
19. S. F. Wu, H. Zhang, B. R. Cairns, *Genome Res.* **21**, 578–589 (2011).
20. T. Cheutin, G. Cavalli, *PLOS Genet.* **8**, e1002465 (2012).
21. A. J. Haigh, W. A. MacDonald, V. K. Lloyd, *Genetics* **169**, 1165–1167 (2005).
22. W. Tadros, H. D. Lipshitz, *Development* **136**, 3033–3042 (2009).
23. S. K. Bowman *et al*., *eLife* **3**, e02833 (2014).
24. M. D. Schroeder, C. Greer, U. Gaul, *Development* **138**, 3067–3078 (2011).
25. F. Pelegri, R. Lehmann, *Genetics* **136**, 1341–1353 (1994).
26. Ö. Copur, J. Müller, *Development* **140**, 3478–3485 (2013).
27. R. Margueron *et al*., *Nature* **461**, 762–767 (2009).
28. H. M. Herz *et al*., *Science* **345**, 1065–1070 (2014).
29. A. Rada-Iglesias *et al*., *Nature* **470**, 279–283 (2011).
30. S. Bonn *et al*., *Nat. Genet.* **44**, 148–156 (2012).
31. E. Z. Kvon *et al*., *Nature* **512**, 91–95 (2014).
32. J. L. Haynie, *Dev. Biol.* **100**, 399–411 (1983).
33. N. J. Francis, N. E. Follmer, M. D. Simon, G. Aghia, J. D. Butler, *Cell* **137**, 110–122 (2009).
34. N. Soshnikova, D. Duboule, *Science* **324**, 1320–1323 (2009).
35. X. Liu *et al*., *Nature* **537**, 558–562 (2016).

ACKNOWLEDGMENTS

We thank the Iovino lab, in particular D. Latreille, D. Ibarra-Morales, and V. Asimi; our colleagues A. Akhtar, T. Jenuwein, P. Becker, R. Sawarkar, E. Trompouki, and especially T. Boehm for critical reading of the manuscript; the Bioinformatics and Sequencing facilities at the Max Planck Institute of Immunobiology and Epigenetics (MPI-IE) (T. Manke, U. Boenisch, L. Arrigoni, and in particular D. Ryan); C. Hug and J. M. Vaquerizas (MPI for Molecular Biomedicine, Muenster, Germany) for initial help in RNA-seq data analysis; S. De Renzis (EMBL) for initial help in staging of the embryos; the Imaging facility, Proteomics facility, and Fly facility at MPI-IE; L. Ringrose and V. Pirrotta for sharing fly stocks; and J. Mueller [E(z)], T. Jenuwein (H3K27me3 and H3K27me2), and the Developmental Studies Hybridoma Bank (Abd-B) for antibodies. The Bloomington *Drosophila* Stock Center (NIH P40OD018537) and the Transgenic RNAi Project at Harvard Medical School (NIH/NIGMS R01-GM084947) provided fly stocks used in this study. Supported by the Max Planck Society and IMPRS program (F.Z. and E.L.); German Research Foundation (DFG) CRC992, Project B06 and Z01 (R.S. and F.K.); Australian Research Council Discovery Early Career Researcher Award DE140101962 (O.B.); and the Max Planck Society and DFG CRC992, Project B06 (N.I.). All the data are deposited at ENA (www.ebi.ac.uk/ena) PRJEB18481 (primary accession), ERP020413 (secondary accession).

SUPPLEMENTARY MATERIALS

www.sciencemag.org/content/357/6347/212/suppl/DC1
Figs. S1 to S5
Tables S1 to S3
Databases S1 to S4
References (*36*–*60*)

5 December 2016; accepted 16 June 2017
10.1126/science.aam5339

Germ line–inherited H3K27me3 restricts enhancer function during maternal-to-zygotic transition

Fides Zenk, Eva Loeser, Rosaria Schiavo, Fabian Kilpert, Ozren Bogdanovic and Nicola Iovino

Science **357** (6347), 212-216.
DOI: 10.1126/science.aam5339

Intergenerational transcription taming

Parents provide genetic information that guides the development of the offspring. Zenk *et al.* show that epigenetic information, in the form of the repressive mark H3K27me3, is also propagated to the offspring and regulates proper gene expression in the embryo. Preventing the propagation of maternally inherited H3K27me3 led to precocious gene activation and, ultimately, embryo lethality.

Science, this issue p. 212